

DIVERSE LONG-TERM VARIABILITY OF FIVE CANDIDATE HIGH-MASS X-RAY BINARIES FROM *Swift* BURST ALERT TELESCOPE OBSERVATIONSROBIN H. D. CORBET^{1,2,3}, JOEL B. COLEY^{4,5}, AND HANS A. KRIMM^{6,7}
(Accepted August 10, 2017)

ABSTRACT

We present an investigation of long-term modulation in the X-ray light curves of five little-studied candidate high-mass X-ray binaries using the *Swift* Burst Alert Telescope. IGR J14488-5942 and AX J1700.2-4220 show strong modulation at periods of 49.6 and 44 days, respectively, which are interpreted as orbital periods of Be star systems. For IGR J14488-5942, observations with *Swift* X-ray Telescope show a hint of pulsations at 33.4 s. For AX J1700.2-4220, 54 s pulsations were previously found with *XMM-Newton*. Swift J1816.7-1613 exhibits complicated behavior. The strongest peak in the power spectrum is at a period near 150 days, but this conflicts with a determination of a period of 118.5 days by La Parola et al. (2014). AX J1820.5-1434 has been proposed to exhibit modulation near 54 days, but the extended BAT observations suggest modulation at slightly longer than double this at approximately 111 days. There appears to be a long-term change in the shape of the modulation near 111 days, which may explain the apparent discrepancy. The X-ray pulsar XTE J1906+090, which was previously proposed to be a Be star system with an orbital period of ~ 30 days from pulse timing, shows peaks in the power spectrum at 81 and 173 days. The origins of these periods are unclear, although they might be the orbital period and a superorbital period respectively. For all five sources, the long-term variability, together with the combination of orbital and proposed pulse periods, suggests that the sources contain Be star mass donors.

Keywords: stars: individual (IGR J14488-5942, AX J1700.2-4220, Swift J1816.7-1613, AX J1820.5-1434, XTE J1906+090) — stars: neutron — X-rays: stars

1. INTRODUCTION

High-mass X-ray Binaries (HMXBs) consist of a neutron star or black hole accreting from an early spectral type (O or B) companion. Mass transfer can occur in a variety of ways, depending on the nature of the mass donor and the orbital separation of the components (e.g. Walter et al. 2015). HMXBs show variability on various timescales, these include the rotation (“pulse”) period of the accreting neutron star and the orbital period.

The largest sub-group of HMXBs is those where accretion occurs from a Be star (e.g. Charles & Coe 2006; Reig 2011). A Be star is a non-supergiant OB star that has, at some time, displayed emission at H α (e.g. Porter & Rivinius 2003). These stars possess a circumstellar “decretion” disk, which is believed to be related to the rapid, but sub-critical, rotation of the star, and possibly also non-radial stellar pulsations (e.g. Rivinius et al. 2013, and references therein). It is from this disk, when it is present, that accretion may occur. The circumstellar disk is not persistent, and may appear and dissipate

on timescales of years. In other HMXBs, accretion takes place from an OB supergiant component and accretion may be either from the stellar wind or, in a small number of systems, via Roche-lobe overflow (e.g. Chaty 2010).

In Be star systems, outbursts can be seen which are generally classified into two categories (e.g. Kretschmar et al. 2012). “Type I” outbursts recur with the orbital period and are expected to occur near periastron passage. “Type II” outbursts, which are irregular and occur less frequently, are more luminous, are not obviously related to the orbital phase, and can have longer durations. The cause of Type II outbursts is unclear, but suspected to be related to the properties of the Be star decretion disk, which is thought to be tidally truncated at a radius resonant with the neutron star orbit (e.g. Reig et al. 2016). Monageng et al. (2017) searched for a correlation between decretion disk size and Type II outbursts from five Be star HMXBs and did not find this. Instead, Monageng et al. (2017) considered other changes in disk properties, precession, elongation and density effects, that could account for Type II outbursts.

It is also possible for a Be star HMXB to show apparently regular outbursts for a time which do not recur on the orbital period. For example, a ~ 80 day period was found in the X-ray flux from XTE J1946+274 by Campana et al. (1999), while pulse timing subsequently showed the orbital period to be ~ 170 days, with the difference in periods perhaps related to an offset between the orbital plane and the plane of the Be star’s decretion disk (Wilson et al. 2003; Marcu-Cheatham et al. 2015).

In Be star systems, long-timescale variations associated with changes in the circumstellar disk may be seen. In all sub-groups of HMXBs, superorbital periods can be seen in some, but not all, systems (e.g. Rajoelimanana et al.

¹ University of Maryland, Baltimore County, MD 21250, USA; corbet@umbc.edu

² CRESST/Mail Code 662, X-ray Astrophysics Laboratory, NASA Goddard Space Flight Center, Greenbelt, MD 20771, USA

³ Maryland Institute College of Art, 1300 W Mt Royal Ave, Baltimore, MD 21217, USA

⁴ NASA Postdoctoral Program, and Astroparticle Physics Laboratory, Code 661 NASA Goddard Space Flight Center, Greenbelt Rd., MD 20771, USA.

⁵ CRESST/Astroparticle Physics Laboratory, Code 661 NASA Goddard Space Flight Center, Greenbelt Rd., MD 20771, USA

⁶ Universities Space Research Association, 10211 Wincopin Circle, Suite 500, Columbia, MD 21044, USA

⁷ National Science Foundation

2011; Corbet & Krimm 2013, and references therein). For Be star systems, at least some of this long term variability may be attributed to one-armed oscillations in the decretion disk (e.g. Okazaki 1991; Ogilvie 2008; Okazaki 2016).

Orbital and long-timescale changes in HMXBs are well suited to study with X-ray all-sky monitors. Such an instrument is the Burst Alert Telescope (BAT) on board the *Swift* satellite (Gehrels et al. 2004), which has now been operating for approximately 12 years. The hard (> 15 keV) X-ray light curves produced by the BAT are particularly important for HMXBs located on the Galactic plane, which can suffer from significant amounts of interstellar and/or local absorption. Light curves from the BAT have enabled the discovery of a number of orbital and super-orbital periods for HMXBs. In our previous work on long-term BAT data we have presented analyses of symbiotic X-ray binaries (Corbet et al. 2008), superorbital modulation in supergiant HMXBs (Corbet & Krimm 2013), and measurements of eclipses in HMXBs (Coley et al. 2015). We routinely monitor BAT light curves, and the power spectra of these, for indications of periodic modulation, particularly for sources located on the Galactic plane. Based on this monitoring, in this paper we select five poorly-studied candidate Be star HMXBs for which the BAT power spectra show features which suggest either orbital, or other types of long-term, modulation. These sources are: IGR J14488-5942, AX J1700.2-4220, Swift J1816.7-1613, AX J1820.5-1434, and XTE J1906+090. These sources display a variety of behavior ranging from apparently clear orbital modulations to more complicated variability.

For none of the sources are there light curves from MAXI (Matsuoka et al. 2009), or *Fermi* Gamma-ray Burst Monitor occultation observations (Wilson-Hodge et al. 2012), and so the BAT provides the only long-term hard X-ray light curves. For AX J1700.2-4220 a long duration X-ray light curve is also available from *Rossi X-ray Timing Explorer (RXTE)* Proportional Counter Array (PCA) observations. Unless otherwise stated, all uncertainties are given at the 1σ level. Preliminary reports of the orbital periods in IGR J14488-5942 and AX J1700.2-4220 appeared in Corbet et al. (2010b), and Corbet et al. (2010a) respectively, but the results presented here are based on light curves covering almost twice the durations of those in the early reports.

2. DATA AND ANALYSIS

2.1. *Swift* BAT Light Curves

The *Swift* BAT is described in detail by Barthelmy et al. (2005), and descriptions of our previous use of data from the BAT can be found in Corbet & Krimm (2013) and Coley et al. (2015). The BAT uses a coded mask to provide a wide field of view (1.4 sr half-coded, 2.85 sr 0% coded), which facilitates its use as an all-sky monitor. The pointing direction of *Swift* is driven by the narrow-field XRT and UVOT instruments on board *Swift*, resulting in the BAT typically observing 50%–80% of the sky each day. We use data from the *Swift* BAT transient monitor (Krimm et al. 2013), which are available shortly after observations have been performed and cover the energy range 15 - 50 keV. In this energy range, the Crab gives

a count rate of $0.22 \text{ cts cm}^{-2} \text{ s}^{-1}$. Transient monitor light curves are available with time resolutions of *Swift* pointing durations (“orbital light curves”), and also daily averages. BAT transient monitor light curves are currently available for 1281 sources. The light curves of the five sources considered here cover the time range of MJD 53,416 to 57,673 (2005-02-15 to 2016-10-12). While BAT light curves are also available from catalogs (e.g. Tueller et al. 2010; Baumgartner et al. 2013), the transient monitor light curves are of much longer duration. As in our previous analyses (Corbet & Krimm 2013; Coley et al. 2015), we used only data for which the data quality flag (“DATA_FLAG”) was 0, indicating good quality and, in addition, removed points with very low fluxes and implausibly small uncertainties from the light curves. Because the BAT pointing direction is primarily driven by XRT and UVOT observations, the observation durations and frequency of durations is variable. The individual observations in the orbital light curves of the five sources have exposures ranging from 64 to 2664 s, with mean exposures of ~ 630 s.

2.2. Period Searches using Power Spectra

Our searches for periodicity in the BAT light curves also followed the procedures described in Corbet & Krimm (2013). Our primary method for searching for periodic modulation is to use discrete Fourier transforms (DFTs) to obtain power spectra. We do not employ the Fast Fourier Transform (FFT) implementation of the DFT. Hence, we use the light curves in their original form and do not require rebinning to a regular grid, or special treatment of data gaps. The uncertainty on individual flux measurements in the light curves can differ greatly due to the range in observation durations, and varied location of sources in the BAT’s field of view. Because of this, the contribution of each data point to the power spectrum is weighted by its uncertainty using the “semi-weighting” technique (Corbet et al. 2007a,b), which takes into account both the error bars on each data point and the excess variability of the light curve. Weighting data points in a power spectrum is analogous to combining individual data points using weighted means (Scargle 1989), and semi-weighting is analogous to using semi-weighted means (Cochran 1937, 1954). We calculated DFTs of the light curves for frequency ranges which correspond to periods of between 0.07 days to the length of the light curves - i.e. generally ~ 4250 days. We oversampled the DFTs by a factor of five compared to their nominal resolution, where we take the nominal frequency resolution to be the inverse of the length of each light curve (e.g. VanderPlas 2017, and references therein). To estimate the significance of peaks in the power spectra we utilize the commonly employed false alarm probability (FAP; Scargle 1982), while we note that possible statistical problems with the FAP have been identified by several authors (e.g. Koen 1990; Baluev 2008; Süveges 2014). We note that the calculation of the FAP can also be complicated if the underlying continuum is not “white”. Attempts to deal with this have employed e.g. the removal of a smoothed continuum (Israel & Stella 1996) or polynomial fits to $\log(\text{power})$ versus $\log(\text{frequency})$ to the entire power spectrum (e.g. Vaughan 2005; Corbet et al. 2008). Here, to estimate FAP values of candidate periods

in the presence of uncertain noise properties of the overall variability, we use the local power level near a peak in the power spectrum derived from a polynomial fit to a limited frequency range. To calculate the FAP, the number of independent frequencies in the total frequency range search should be known which depends on the frequency resolution. While this is not precisely defined for unevenly sampled data (e.g. Koen 1990), we have previously found that using the inverse of the light curve length provides a reasonable approximation (Corbet et al. 2008). Uncertainties in periods are generally derived using the expression of Horne & Baliunas (1986), again using the local power level rather than the mean of the total power spectrum. We do not apply a barycentric correction to the observation times for the analysis presented here. In all cases, barycentric corrections would be much smaller than uncertainties on the periods considered.

A DFT based approach to period searching is most sensitive to sinusoidal modulation. Modulation such as a repetitive flare that is limited to a brief orbital phase will result in the modulation being spread over many harmonics in the power spectrum. While this can be alleviated by summing a certain number of harmonics (e.g. Buccheri et al. 1983), we do not generally see sharp flaring in our sources and do not employ this here. While period searches based on folding may be more sensitive to brief flare-like behavior, we note though that folding techniques can result in spurious signals at “sub-harmonics” that do not occur in Fourier-based analyses.

2.3. *Period Persistence Tests: Dynamic Power Spectra, Time-Slice Folds, and Height vs. Time Plots*

To investigate the persistence of a possible signal, it can be illustrative to investigate changes in the power spectrum of a light curve as a function of time. In this case, power spectra are calculated of temporal subsets of the light curve, potentially with overlap between subsets. Images of the power spectrum as a function of time can then be instructive about changes in modulation, and appearance and disappearance of signals. However, the periods of the sources discussed here are relatively long compared to the total light curve length, and may also require a light curve subset that is a significant fraction of the total length in order to be detected. For the dynamic power spectra, it is therefore often required to use overlapping light curve subsets that are not statistically independent. The length of the temporal subsets, and the degree of overlap, are not naturally defined and must be selected by a user.

We also employ simple folding of light curve subsets on periods obtained from the entire light curve, but selecting temporal subsets of the light curve which have no overlap. The length we choose for the subset light curves varies from source to source, and depends on factors including the strength of the modulation.

In addition, we can investigate the change in strength of the modulation at a particular period as a function of time. For a persistent coherent modulation with constant level of modulation, an approximately linear change in peak power relative to the average power with time is expected. Changes in the gradient of the change in signal strength can thus reveal times when signal strength was relatively stronger or weaker.

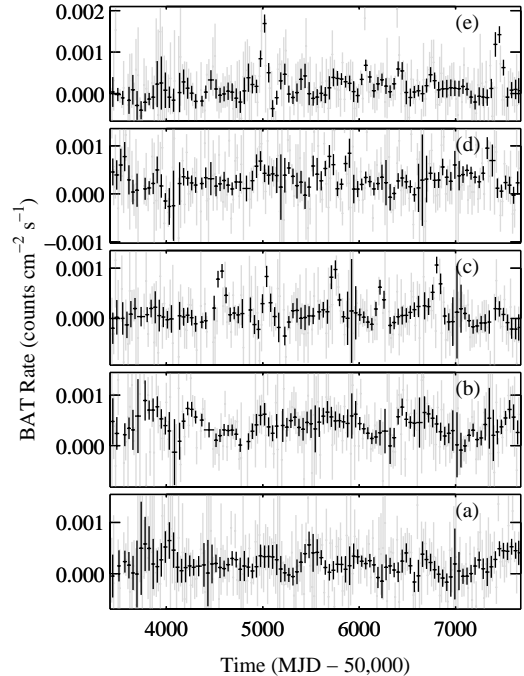


Figure 1. BAT light curves of: (a) IGR J14488-5942, (b) AX J1700.2-4220, (c) Swift J1816.7-1613, (d) AX J1820.5-1434, and (e) XTE J1906+090. The gray points show light curves derived from the one day average light curves, rebinned to a time resolution of 21 days. The black points are rebinned to a time resolution of 42 days, then smoothed by convolution with a triangular response of full-width half maximum of 84 days.

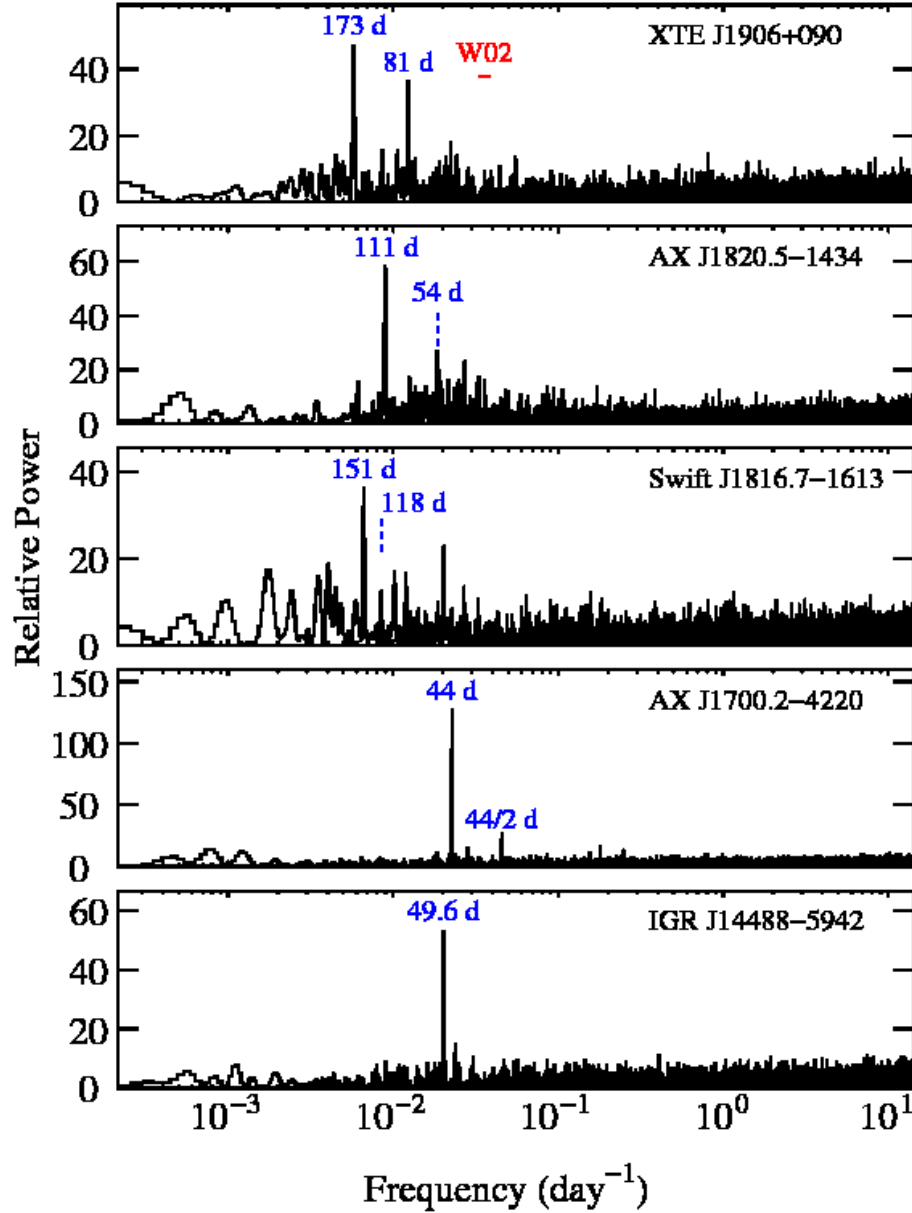


Figure 2. Power spectra of the BAT light curves of IGR J14488-5942, AX J1700.2-4220, Swift J1816.7-1613, AX J1820.5-1434, and XTE J1906+090. For each source candidate periods are marked. For Swift J1816.7-1613 the dashed lines mark the 118 and 151 day periods reported by La Parola et al. (2014) and Corbet & Krimm (2014) respectively. For AX J1820.5-1434 the dashed line marks the 54 day period reported by Segreto et al. (2013). The highest peak in the power spectrum is at a period of ~ 111 days. For XTE J1906+090 the two highest peaks at ~ 173 and 81 days are marked. The short horizontal line marked “W02” is the 26–30 day period range suggested by Wilson et al. (2002) from pulse timing. See text for additional details.

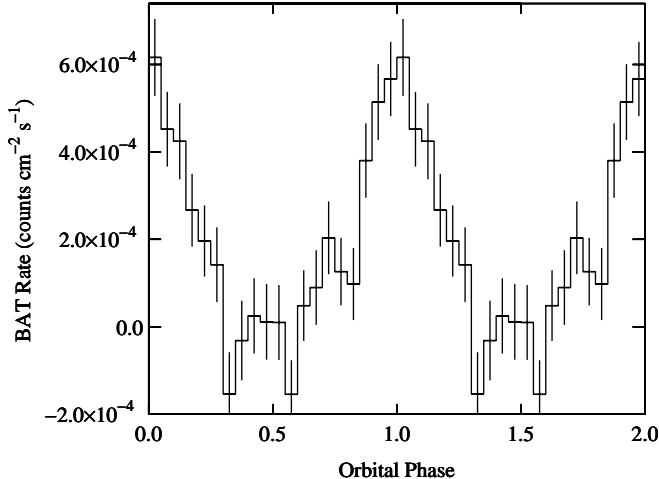


Figure 3. BAT light curve of IGR J14488-5942 folded on the proposed 49.63 day orbital period. Phase 0 corresponds to MJD 56,054.5.

3. SOURCES AND ANALYSIS RESULTS

3.1. IGR J14488-5942

IGR J14488-5942 was first listed in the 4th INTEGRAL/IBIS Survey Catalogue (Bird et al. 2010) as a variable source. Although it was not present in the BAT 22 month survey (Tueller et al. 2010), it is present in the 70 month catalog (Baumgartner et al. 2013) as Swift J1448.4-5945. Landi et al. (2009) performed *Swift* XRT observations covering the location of IGR J14488-5942 and found two sources: “N1” and “N2”. They proposed that the brighter and spectrally harder source, N2 (Swift J144843.3-594216), was the counterpart of IGR J14488-5942. Rodriguez et al. (2010) also analyzed the *Swift* XRT observations and also slightly preferred the brighter source as the counterpart, in which case it could be a highly-absorbed X-ray binary. From optical spectroscopy, Coleiro et al. (2013) suggested that the system is more likely to contain a Be star primary than a supergiant.

3.1.1. BAT Observations of IGR J14488-5942

The BAT light curve of IGR J14488-5942 is shown in Figure 1(a). The mean count rate is $(1.9 \pm 0.2) \times 10^{-4}$ cts $\text{cm}^{-2} \text{s}^{-1}$ (~ 0.9 mCrab). The power spectrum of the light curve for periods longer than 0.07 days is shown in Figure 2. A single highly significant peak is seen near 49.6 days. The false alarm probability is $< 10^{-6}$. The period is 49.63 ± 0.05 days. This is consistent with, but more precise than, the value of 49.51 ± 0.12 d given in Corbet et al. (2010b). The folded light curve is shown in Figure 3, and it shows an approximately sinusoidal modulation. From a sine wave fit to the light curve we derive an epoch of maximum flux of $\text{MJD } 56,054.5 \pm 0.7$. The change of the peak height at 49.63 days in the power spectrum shows a fairly constant increase with time (Figure 4) suggesting that modulation at this period is a persistent property of the light curve.

3.1.2. Swift XRT Observations of IGR J14488-5942

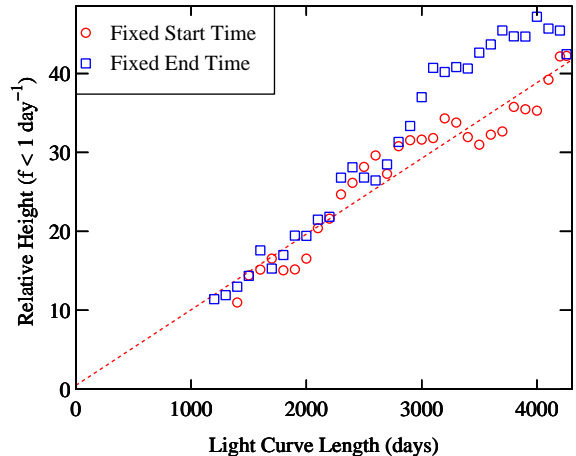


Figure 4. Relative height of the peak near 49.6 days in the power spectrum of the BAT light curve of IGR J14488-5942 as a function of light curve length. Red circles indicate light curves which all have the same start time (MJD 53,416), and blue squares are light curves with the same end time (MJD 57,673).

The *Swift* XRT observations of IGR J14488-5942 described by Landi et al. (2009) and Rodriguez et al. (2010) were obtained on 2009-09-25 (MJD 55,099) with an exposure time of ~ 16.4 ks. Two sources were detected in the region, the brighter source is Swift J144843.3-594216 (“Src #1” in Rodriguez et al. 2010, “N2” in Landi et al. 2009) and the fainter source is Swift J144900.5-594503 (“Src #2” in Rodriguez et al. 2010, “N1” in Landi et al. 2009). The time of the XRT observations corresponds to a phase of 0.93 when IGR J14488-5942 would be expected to be bright. The XRT data were obtained in photon-counting (PC) mode which has a time resolution of 2.5 s. We extracted XRT light curves using aperture photometry, with aperture radii of $1.25'$, following the procedures described in the *Swift* XRT Data Reduction Guide (Capaldi et al. 2005). For the brighter source, Swift J144843.3-594216, the non-background subtracted count rate in the aperture was $0.25 \text{ counts s}^{-1}$ and for the fainter source, Swift J144900.5-594503, it was $0.004 \text{ counts s}^{-1}$. We searched for pulsations for periods longer than 10 s in both sources. No pulsations were seen in Swift J144843.3-594216. For the fainter source, Swift J144900.5-594503, a marginal signal was seen at a period of 33.419 ± 0.001 seconds with an FAP of $\sim 1.4\%$ (Figure 5). The XRT light curve folded on this period is also shown in Figure 5.

3.2. AX J1700.2-4220

AX J170017-4220 was included in a list of faint X-ray sources found in a survey of the Galactic plane with ASCA (Sugizaki et al. 2001). This source is then listed, as AX J1700.2-4220, as a counterpart to a source in the first INTEGRAL catalog (Bird et al. 2004). From CTIO 1.5 m telescope optical spectroscopy, Masetti et al. (2006) tentatively identified the Be star HD 153295, which lies within the INTEGRAL error region, but outside the smaller ASCA error region, as the counterpart. Negueruela & Schurch (2007) presented intermediate-resolution optical spectroscopy, obtained with the 1.9m

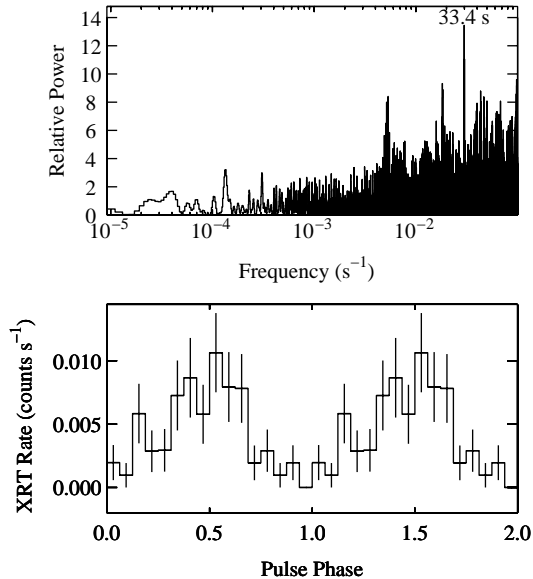


Figure 5. Top: Power spectrum of the Swift XRT light curve of IGR J14488-5942 possible counterpart Swift J144900.5-594503. Bottom: XRT light curve of Swift J144900.5-594503 folded on the possible 33.4 s pulse period.

telescope at the South African Astronomical Observatory, and derived a spectral type of B0.5 IVe. *Chandra* observations by Anderson et al. (2014) confirmed the identification of AX J1700.2-4220, via the detection of a source which they termed ChI J1700174220_1, with HD 153295. Anderson et al. (2014) also noted that HD 153295 had unusual near-infrared colors.

3.2.1. BAT Observations of AX J1700.2-4220

The BAT light curve of AX J1700.2-4220 is shown in Figure 1(b). The mean count rate is $(3.9 \pm 0.2) \times 10^{-4}$ cts $\text{cm}^{-2} \text{s}^{-1}$ (~ 1.8 mCrab). The power spectrum of the light curve is shown in Figure 2. A highly significant peak is seen near 44 days, together with a significant peak at the second harmonic of this. The false alarm probability is $< 10^{-6}$ and the period is 44.03 ± 0.03 days. This period is consistent at the $\sim 2 \sigma$ level with, but more precise than, the value of 44.12 ± 0.04 days given in Corbet et al. (2010a). The folded light curve is shown in Figure 6, and the folded profile is roughly sinusoidal, although perhaps with a somewhat slower rise to maximum than subsequent decline. From a sine wave fit to the light curve, we derive an epoch of maximum flux of MJD $56,059.2 \pm 0.4$.

The change of the peak height near 44 days in the power spectrum (Figure 7), shows an initially faster increase with increasing light curve length than for later in the light curve. This suggests that, although modulation near 44 days is a persistent property of the light curve, it was more prominent for the first ~ 1000 days (MJD 53,416 to $\sim 54,400$). The dynamic power spectrum of the BAT light curve (Figure 8) is also consistent with the modulation being stronger for the earlier portion of the light curve. We divided the entire light curve into

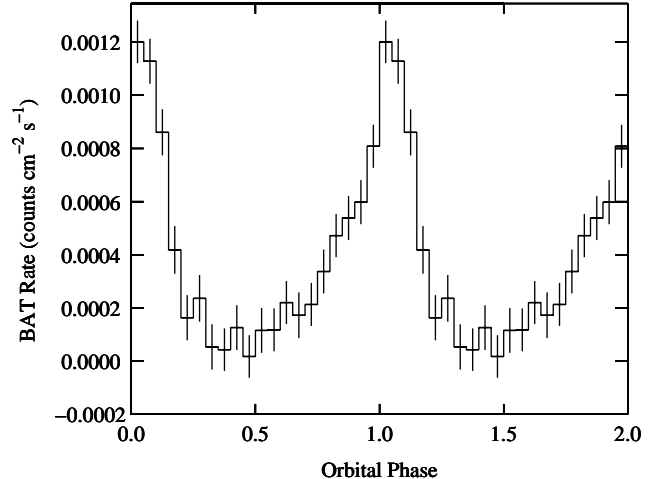


Figure 6. BAT light curve of AX J1700.2-4220 folded on the proposed 44.03 day orbital period. Phase 0 corresponds to MJD 56,059.2.

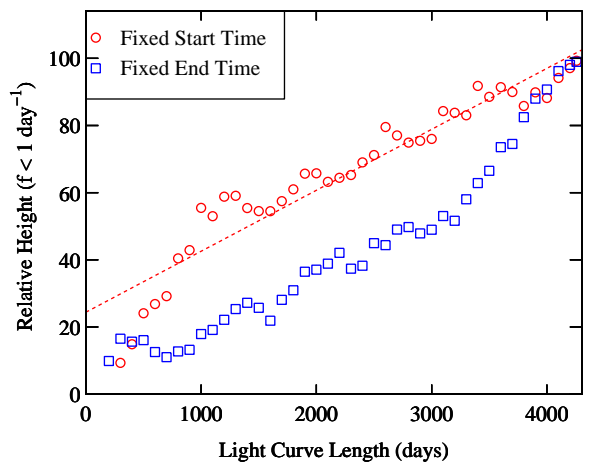


Figure 7. Relative height of the peak near 44 days in the power spectrum of the BAT light curve of AX J1700.2-4220 as a function of light curve length. Red circles indicate light curves which all have the same start time (MJD 53,416), and blue squares are light curves with the same end time (MJD 57,673).

five equal length sections and folded each on the 44 day period, and this is shown in Figure 9. This shows that the modulation persists throughout the light curve, although the source is brightest and shows the strongest modulation at earliest times.

3.2.2. RXTE Observations of AX J1700.2-4220

Long-term observations of sources near the Galactic center are available from scans across this region made with the *RXTE* PCA (Swank & Markwardt 2001), and cover an energy range of 2 - 10 keV. Detection of the orbital period of AX J1700.2-4220 from *RXTE* PCA Galactic plane observations was reported by Markwardt et al. (2010), who obtained a period of 44.03 ± 0.14 days. We investigate here the full PCA light curve that covers the time range 2004-06-10 (MJD 53,166) to 2011-10-29

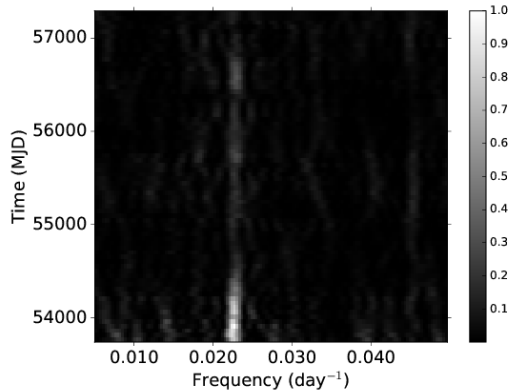


Figure 8. Power spectrum of the BAT light curve of AX J1700.2-4220 as a function of time. The low and high frequencies correspond to periods of 200 and 20 days, respectively. The power spectra were calculated for light curve segments of length 650 days, with increments in start and end times of the segments of 50 days. The power spectra are normalized to the maximum power at any time.

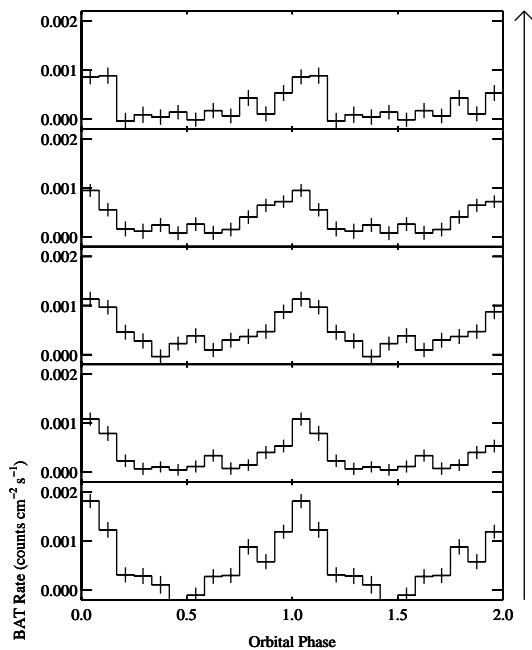


Figure 9. Light curve of BAT light curve of AX J1700.2-4220 divided into equal length (851 day) sections, and each folded on the 44.03 day period. The arrow indicates increasing time. Phase 0 corresponds to MJD 56,059.2.

(MJD 55,863), which is $\sim 25\%$ longer than that available to Markwardt et al. (2010). The power spectrum of the PCA light curve is shown in Figure 10. The orbital period derived from the PCA scan light curve is 43.98 ± 0.07 days, which is consistent with the period derived with the BAT. The PCA light curve folded on the presumed orbital period is also shown in Figure 10. This appears similar to the folded BAT light curve. The lowest flux counts have negative values, which are likely due to the flux bias noted by Markwardt et al. (2010).

We also examined the 1.5 - 12 keV *RXTE* All-sky Monitor (Levine et al. 1996) light curve of AX J1700.2-4220 which covers the time range MJD 50,088 to 55,813 (1996-

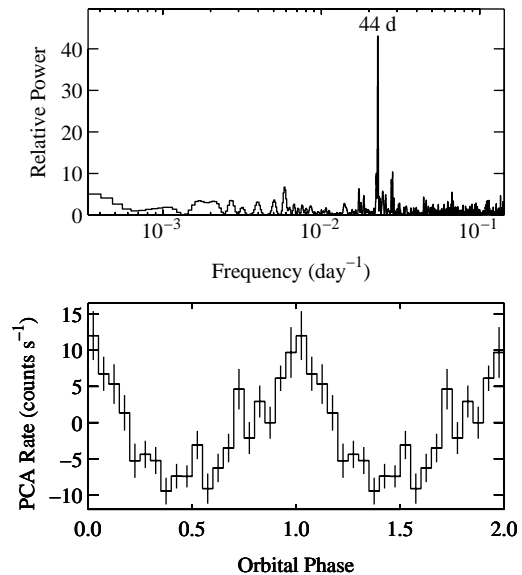


Figure 10. Top panel: Power spectrum of the PCA light curve of AX J1700.2-4220. Bottom panel: PCA light curve of AX J1700.2-4220 folded on the proposed 44.03 day orbital period. Phase 0 corresponds to MJD 56,059.2.

01-06 to 2011-09-09). The power spectrum of this shows no evidence for modulation on the 44 day period.

3.3. BAT Observations of *Swift* J1816.7-1613

The transient X-ray source *Swift* J1816.7-1613 was discovered with the *Swift* BAT by Krimm et al. (2008). A pulse period of 143 s was found by Halpern & Gotthelf (2008) from *Chandra* observations, and this was confirmed by Krimm et al. (2013) from *RXTE* PCA data. Analysis of archival BeppoSAX data also indicated an earlier detection of the source (Orlandini & Frontera 2008). Corbet & Krimm (2014) proposed a possible orbital period of 151.4 ± 1 days using *Swift* BAT data. However, La Parola et al. (2014) reported the detection of a 118.5 ± 0.8 day period, also from BAT data, but using only data obtained around the time of apparent flares in the light curve. No optical counterpart has so far been identified. However, Corbet & Krimm (2014) and La Parola et al. (2014) both suggested a Be star classification based on the location of the source in the spin/orbital period diagram (Corbet 1986) for their proposed orbital periods.

The BAT light curve of *Swift* J1816.7-1613 is shown in Figure 1(c), the power spectrum of this is shown in Figure 2. The mean count rate is $(1.1 \pm 0.2) \times 10^{-4}$ cts $\text{cm}^{-2} \text{s}^{-1}$ (~ 0.5 mCrab). The strongest peak is at a period of 151.1 ± 0.5 days, which is consistent with the 151.4 ± 1 day period reported in Corbet & Krimm (2014). Although the peak height is ~ 36 times larger than the mean power level, the noise level near this peak appears higher. Using a 2nd order polynomial fit to obtain the local power, the relative height is ~ 8 times the local power level, and so is not statistically significant. The 118 day period reported by La Parola et al. (2014),

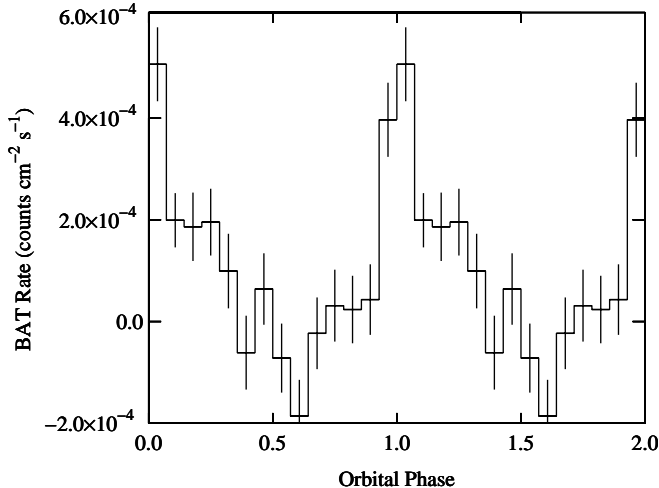


Figure 11. BAT light curve of Swift J1816.7-1613 folded on a period of 151.1 days. Phase 0 corresponds to MJD 56,967.

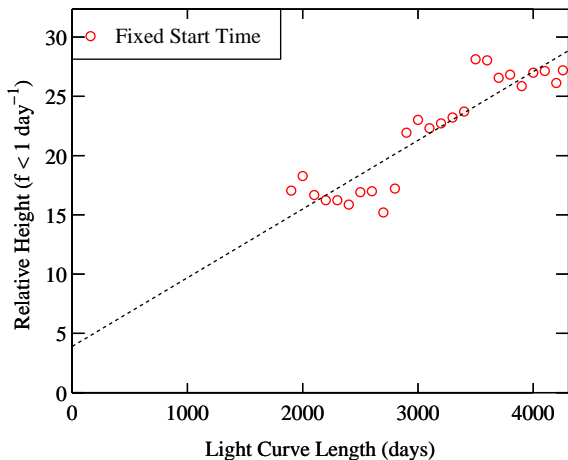


Figure 12. Relative height of the peak near 151 days in the power spectrum of the BAT light curve of Swift J1816.7-1613 as a function of light curve length with all light curves having a start time of MJD 53,416.

based on selected subsets of the light curve, is not detected in the power spectrum of the entire light curve. In Figure 11 we show the BAT light curve folded on the 151.1 period, with an assumed epoch of maximum flux of MJD 56,967. This shows an apparently fairly sharply peaked profile. A plot of height of the peak in the power spectrum at this period with time (Figure 12) shows that while there is a general trend to increase with time, the height does not increase consistently. Folding sections of the BAT light curve on the 151.1 day period (Figure 13), shows that the modulation is most clearly seen in the most recent quarter (1064 days) of the light curve.

We also calculated the power spectrum of Swift J1816.7-1613 using only the restricted time ranges adopted by La Parola et al. (2014) and this is shown in Figure 14. The maximum in the power spectrum is at a period of 118.9 ± 0.6 days which is

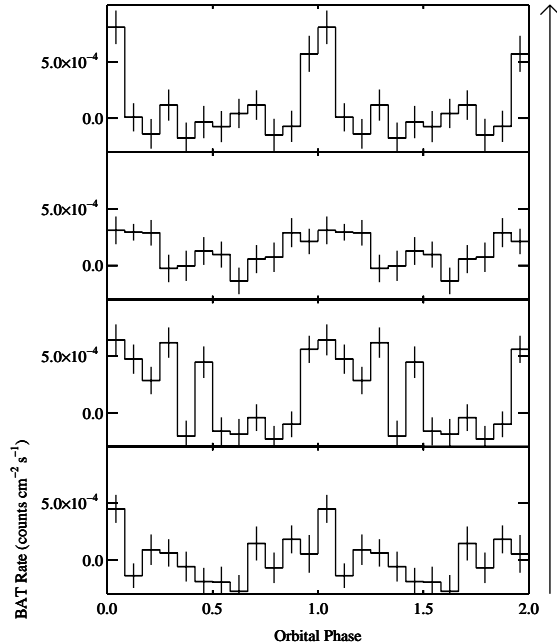


Figure 13. Light curve of BAT light curve of Swift J1816.7-1613 divided into equal length (1064 day) sections, and each folded on the possible 151.1 day period. The arrow indicates increasing time. Phase 0 corresponds to MJD 56,967.

consistent with the period of 118.5 ± 0.8 days found by La Parola et al. (2014). We note that by selecting only time ranges around a modest number of apparent flares, six gaps of length ~ 140 to 500 days are created in the light curve. These gaps have the potential to cause “aliases” in power spectra and other period search techniques. To investigate this, we created light curves based on the BAT light curve times, but with the data values replaced with sine wave modulations at 151.1 and 118.5 days. In both cases aliasing created small peaks at the other period (Figure 15).

3.4. BAT Observations of AX J1820.5-1434

AX J1820.5-1434 was discovered by Kinugasa et al. (1998) during a survey of the Galactic plane using ASCA, and a pulse period of 152.26 ± 0.04 s was measured. Searches for an optical counterpart have not yet resulted in a definite identification (Kaur et al. 2010; Negueruela & Schurch 2007). The source has been detected with *INTEGRAL* (Lutovinov et al. 2003, 2005; Bird et al. 2010) and, from flaring activity seen with this satellite, Walter & Zurita Heras (2007) tentatively suggested that the source was a Supergiant Fast X-ray Transient (SFXT). Segreto et al. (2013) reported the determination of a 54.0 ± 0.4 day orbital period for AX J1820.5-1434 from an analysis of *Swift* BAT observations obtained up to March 2012 (\sim MJD 56,000) and suggested that this may be a Be star system. Segreto et al. (2013) also considered whether changes in source variability might indicate that the recurrent flaring on the 54 day period might *not* be related to periastron passages. The identification of the 54 day period by Segreto et al. (2013) used a folding technique, and so sub-harmonics of their period were also present in their periodogram.

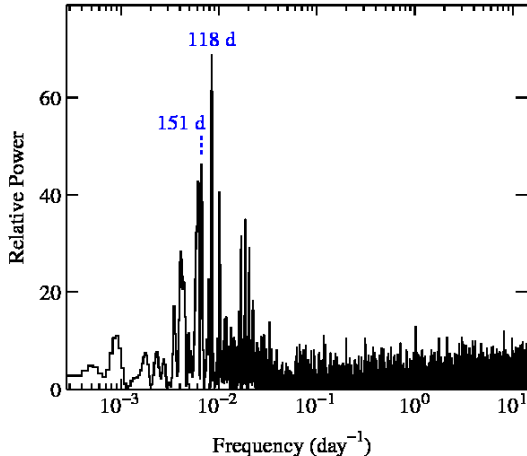


Figure 14. Power spectrum of the BAT light curve of Swift J1816.7-1613 using only the time ranges adopted by La Parola et al. (2014) around candidate flares.

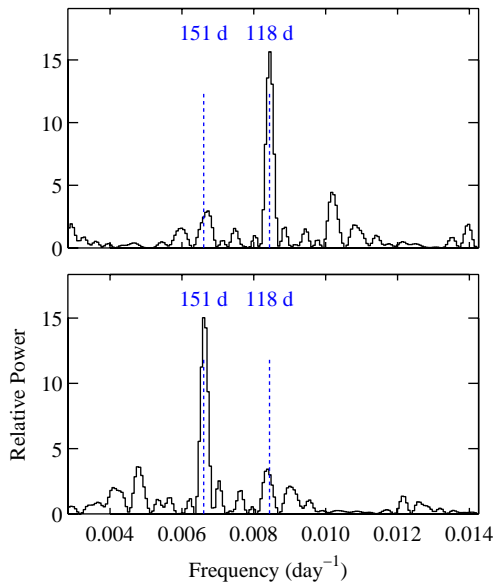


Figure 15. Power spectra of light curves with sine waves with periods of 151.1 days (bottom) and 118.5 days (top) using data times from the BAT light curve of Swift J1816.7-1613 using only the time ranges adopted by La Parola et al. (2014) around candidate flares.

The BAT light curve of AX J1820.5-1434 is shown in Figure 1(d), and the power spectrum of this is plotted in Figure 2. The mean count rate is $(2.9 \pm 0.2) \times 10^{-4}$ cts $\text{cm}^{-2} \text{s}^{-1}$ (~ 1.3 mCrab). The strongest peak in the power spectrum is at a period of 111.8 ± 0.3 days. While the peak is ~ 58 times the mean power level, it is only ~ 11 times the local power level. The 111.8 day period is approximately, although formally inconsistent with, twice the period of 54.0 ± 0.4 days reported by Segreto et al. (2013). The second strongest peak in the

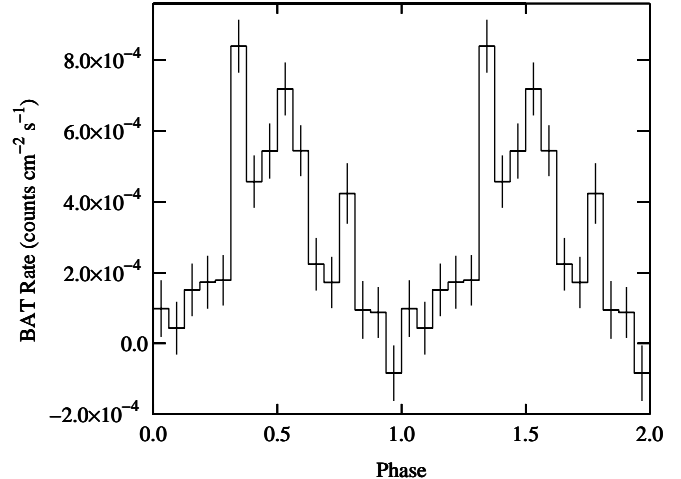


Figure 16. BAT light curve of AX J1820.5-1434 folded on the possible 111.8 day period. Phase 0 corresponds to MJD 54,684.809 (Segreto et al. 2013).

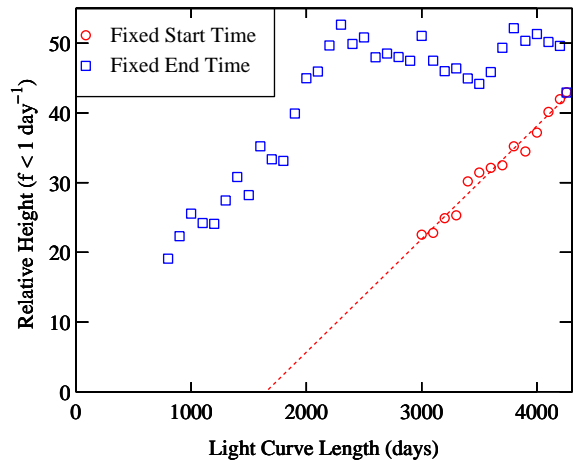


Figure 17. Relative height of the peak near 111 days in the power spectrum of the BAT light curve of AX J1820.5-1434 as a function of light curve length. Red circles indicate light curves which all have the same start time (MJD 53,416), and blue squares are light curves with the same end time (MJD 57,673).

power spectrum has a much lower amplitude and is at 54.1 ± 0.1 days. This small peak would be consistent with the Segreto et al. (2013) period, but is not consistent with the second harmonic of the 111.8 day period. The BAT light curve folded on the 111.8 day period is shown in Figure 16. We note that the profile, while having an overall smooth modulation, is rather “jagged” with bin-to-bin variability.

From the plot of relative peak height near 111.8 days against time (Figure 17), a steady increase in peak height can be seen, but the extrapolation back to a relative peak height of zero starts at approximately 1650 days after the start of the light curve (\sim MJD 55,066). For a similar approach, but using increasing length light curves that always *end* at the time of the last observation (MJD 57,673) we find that the relative peak height

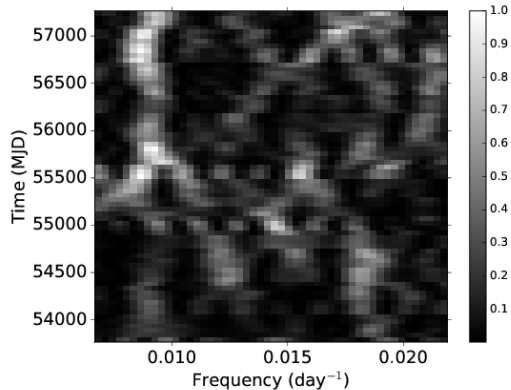


Figure 18. Power spectrum of the BAT light curve of AX J1820.5-1434 as a function of time. The low and high frequencies correspond to periods of 150 and 45 days, respectively. The power spectra were calculated for light curve segments of length 700 days, with increments in start and end times of the segments of 50 days. The power spectra are normalized to the maximum power at any time.

initially steadily increases as earlier start times are used. However, the relative peak height reaches a maximum then roughly plateaus for a light curve start time of ~ 2300 days before the end of the light curve. i.e. for times earlier than \sim MJD 55,370. This suggests that the periodic modulation of the light curve became significantly stronger at some time near MJD 55,200. The dynamic power spectrum of AX J1820.5-1434 (Figure 18) is also suggestive of modulation near 111.8 days ($f \sim 0.009$ day $^{-1}$) becoming apparent after \sim MJD 55,200. We show in Figure 19 the light curve divided into equal length sections folded on the 111.8 day period. From this it can be seen that earlier time data shows a more strongly multi-peaked profile than do later sections of the data.

3.5. BAT Observations of XTE J1906+090

Marsden et al. (1998) serendipitously discovered the transient 89 s pulsar XTE J1906+090 (= XTE J1906+09) during *RXTE* PCA observations of the nearby source SGR 1900+14. From pulse timing, Wilson et al. (2002) suggested an orbital period in the range of 26–30 days. Wilson et al. (2002) noted that this combination of pulse and orbital periods would make the system an outlier from the correlation between these periods found for Be systems (Corbet 1984, 1986). From Chandra observations, Göğüş et al. (2005) identified optical and infrared counterparts which they claimed, based on the optical and infrared colors, added to the evidence that XTE J1906+090 is a transient Be star X-ray binary.

The light curve of XTE J1906+090 is plotted in Figure 1 (e), and the power spectrum of this is shown in Figure 2. The mean count rate is $(1.0 \pm 0.2) \times 10^{-4}$ cts cm $^{-2}$ s $^{-1}$ (~ 0.5 mCrab). No peak is seen in the period range of 26 - 30 days suggested by Wilson et al. (2002) from pulse timing. Instead, the two strongest peaks are seen at periods of 173.1 ± 0.6 days and 81.4 ± 0.1 days. We note that these periods are *not* consistent with being harmonics of each other. In Figures 20 and 21 we show the BAT light curve folded on the 173.1 and 81.4 day periods, respectively. The light curve folded on the 173.1 day period shows sharply peaked modulation, while the data folded on 81.4 days shows a smoother modulation. In Figure 23 we plot the changes in relative peak heights as a function

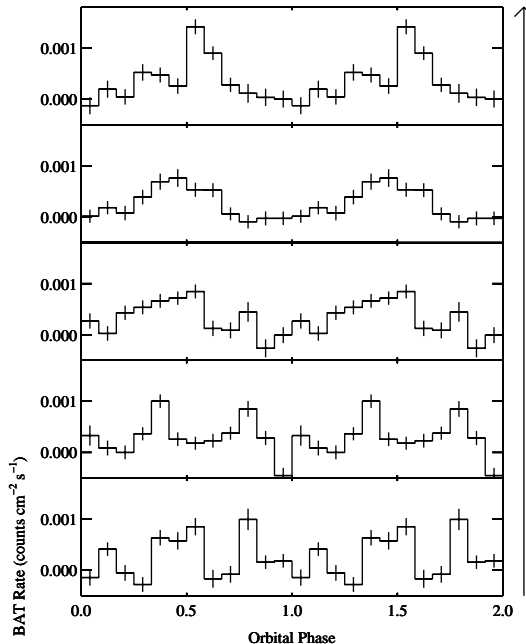


Figure 19. Light curve of BAT light curve of AX J1820.5-1434 divided into equal length (851 day) sections, and each folded on the 111.8 day period. The arrow indicates increasing time. Phase 0 corresponds to MJD 54,684.809 (Segreto et al. 2013).

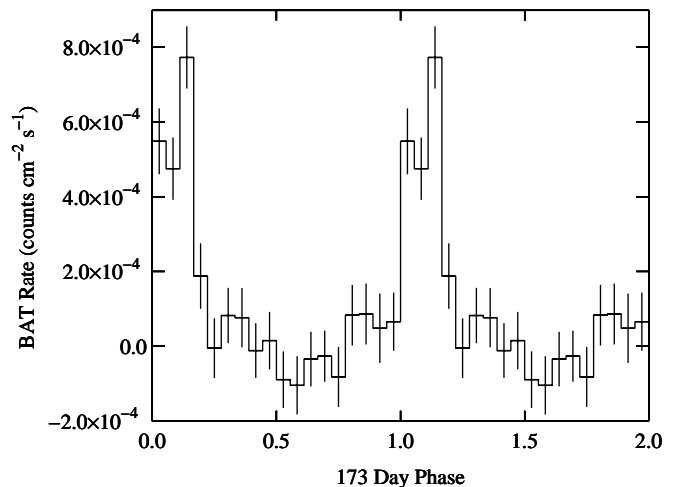


Figure 20. BAT light curve of XTE J1906+090 folded on the 173.1 day peak in the power spectrum. Phase 0 corresponds to MJD 55,000.

of increasing light curve length. For both possible periods, although the tendency is for peak height to increase with time, the increases are rather erratic.

In Figure 22 we show the light curve folded on the 81.4 day period with data selected on two phase intervals of the 173 day period to correspond to bright and faint phases of that possible modulation. As would be expected, the data from the brighter phase has a higher flux level. In addition, the modulation appears stronger during the brighter phase, with an apparent appearance of a secondary peak offset by about 0.5 in phase from the

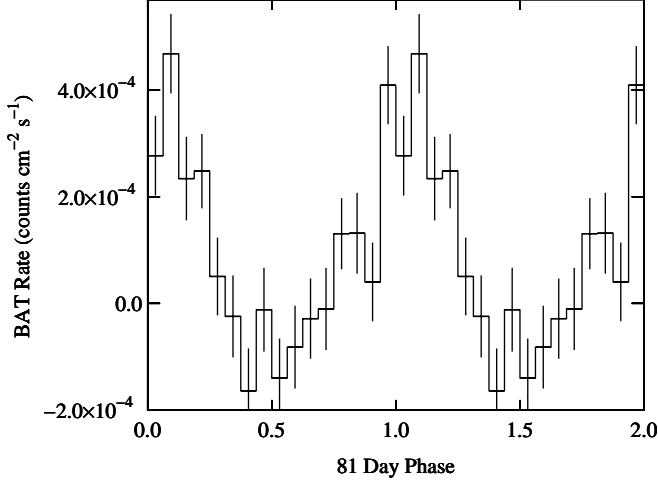


Figure 21. BAT light curve of XTE J1906+090 folded on the 81.4 day peak in the power spectrum. Phase 0 corresponds to MJD 55,000.

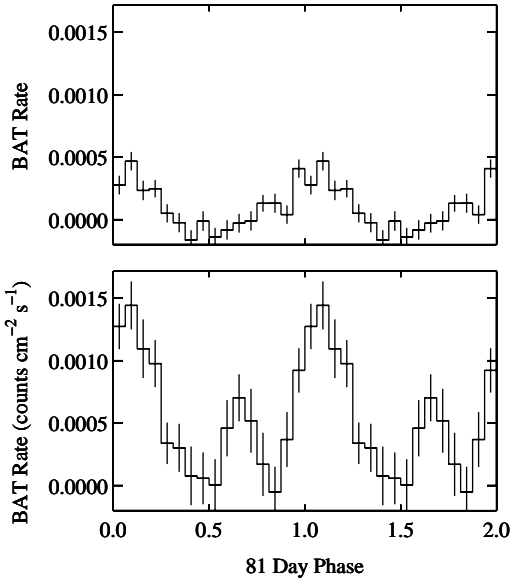


Figure 22. BAT light curves of XTE J1906+090 folded on the 81.4 day peak in the power spectrum selected by phase of the 173.1 day modulation. Top: phases 0.15 to 1.0. Bottom: phases 0.0 to 0.15. Phase 0 corresponds to MJD 55,000 for both the 81.4 and 173 day modulation.

primary peak.

We note the presence in the long-term light curve (Figure 1(e)) of two bright states/flares at approximately MJD 55,000 and 57,450. If data around these times are removed, then the power spectrum still has a maximum at ~ 173 days, although at considerably reduced power.

In Figure 24 we show the dynamic power spectrum of the BAT light curve for XTE J1906+090. The onset of modulation at both ~ 81 and 173 days appears to be associated with the first flare in the light curve. In Figures

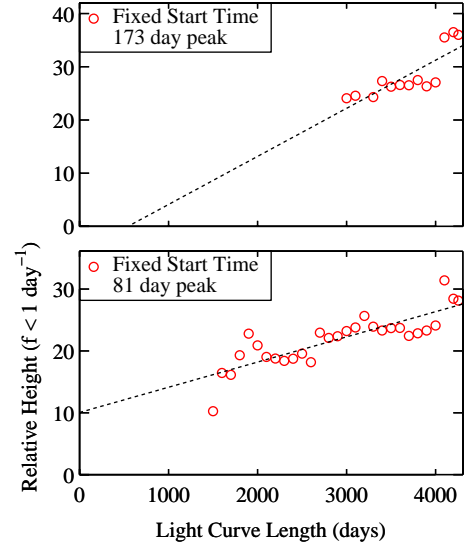


Figure 23. Bottom panel: Relative height of the peak near 81 days in the power spectrum of the BAT light curve of XTE J1906+090 as a function of light curve length, with all light curves having a start time of MJD 53,416. Top panel: Relative height of the peak near 173 days in the power spectrum of the BAT light curve of XTE J1906+090 as a function of light curve length, with all light curves having a start time of MJD 53,416.

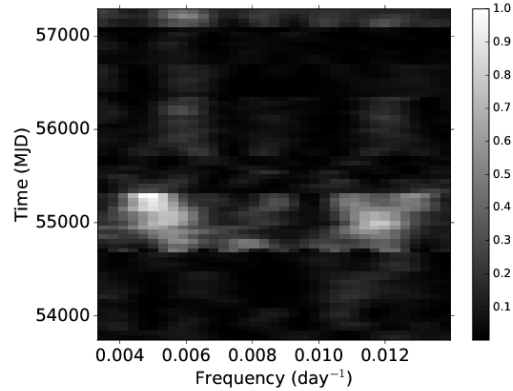


Figure 24. Power spectrum of the BAT light curve of XTE J1906+090 as a function of time. The low and high frequencies correspond to periods of 300 and 70 days, respectively. The power spectra were calculated for light curve segments of length 650 days, with increments in start and end times of the segments of 50 days. The power spectra are normalized to the maximum power at any time.

25 and 26 we show the light curve divided into equal length sections folded on the 81.4 and 173.1 day periods, respectively. These are also suggestive of increased modulation on these periods at later times.

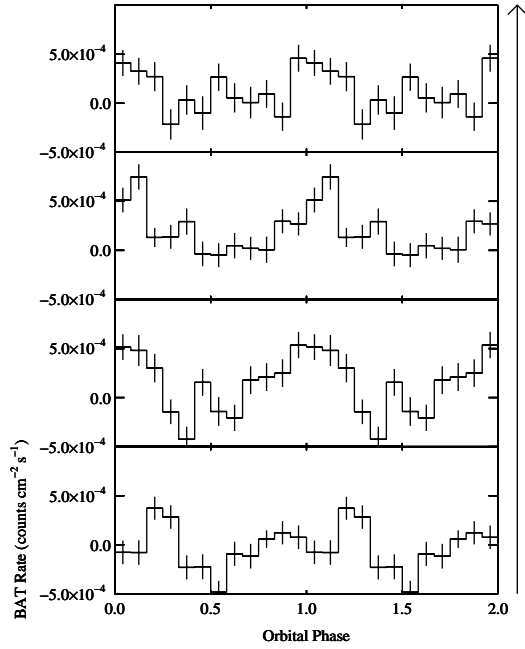


Figure 25. Light curve of BAT light curve of XTE J1906+09 divided into equal length (1064 day) sections, and each folded on the 81.4 day period. The arrow indicates increasing time. Phase 0 corresponds to MJD 55,000.

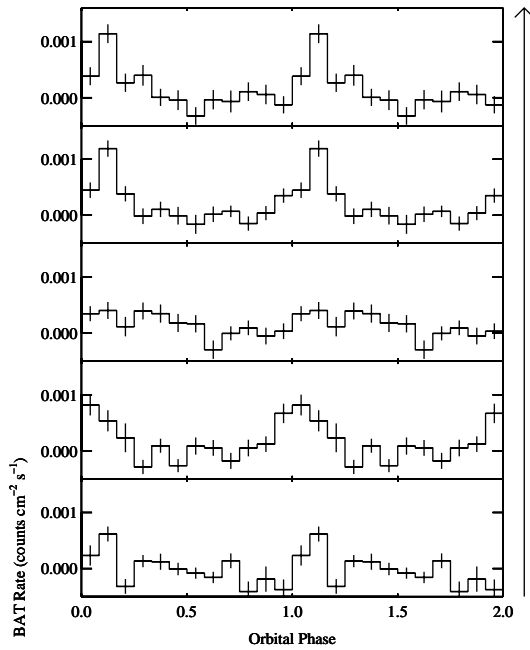


Figure 26. Light curve of BAT light curve of XTE J1906+09 divided into equal length (851 day) sections, and each folded on the 173.1 day period. The arrow indicates increasing time. Phase 0 corresponds to MJD 55,000.

4. DISCUSSION

Even without an optical counterpart, the likely nature of the mass donor in an HMXB can often be inferred from the length of the orbital period, and the nature of the orbital modulation. The inferences can generally be stronger if a measurement of neutron star rotation period is also available (Corbet 1986, and Figure 27 this work). The pulse periods of wind-accretion supergiant systems are generally rather long ($\gtrsim 100$ s), with relatively short orbital periods ($\lesssim 20$ days). Roche-lobe overflow powered HMXBs are highly luminous, with rather short pulse periods. Be star systems have longer orbital periods ($\gtrsim 20$ days), and exhibit a range of pulse periods that, while correlated with orbital period (Corbet 1984, 1986), exhibit considerable scatter around the correlation line. The Be system SAX J2103.5+4545, in particular, is located far from the general correlation trend with a short orbital period, but a relatively long spin period, more typical of a wind accretion supergiant system (e.g. Reig et al. 2010, and references therein). For Be star systems, there also appears to be a bimodal distribution of spin and orbital periods (Knigge et al. 2011) which has been attributed to the neutron stars being formed in two types of supernova (Knigge et al. 2011) or differences in accretion modes (Cheng et al. 2014).

Analysis of the BAT light curves for IGR J14488-5942 and AX J1700.2-4220 shows strong persistent modulation at periods of 49.6 and 44 days, respectively, which are naturally interpreted as the orbital periods of these systems. The lengths of the orbital periods suggest that the modulations are “Type I” outbursts from Be star systems that occur near periastron passage. For IGR J14488-5942, the possible 33.4 s pulse period in the *Swift* XRT data would be consistent with the Be star pulse/orbital period correlation (Figure 27) for a 49.6 day orbital period. However, the significance of the modulation is very low, and is found for the fainter source in the region which previous authors considered to be the less likely counterpart (Landi et al. 2009; Rodriguez et al. 2010). Additional observations are therefore required to determine the reality of the candidate pulse period, and to search for shorter periods for both XRT sources in the region than was possible with the 2.5s time resolution. For AX J1700.2-4220, the 54 s pulse period found by Markwardt et al. (2010), combined with the 44 day period again clearly place the source in the Be star region of the pulse/orbital period diagram (Figure 27).

For *Swift* J1816.7-1613, AX J1820.5-1434, and XTE J1906+090 the situation is more complicated. All three of these sources are pulsars, and the expectation is that they are probably Be star sources. While all three show at least one prominent peak in their power spectra, there can be problems in interpreting these as the orbital periods of these systems.

For *Swift* J1816.7-1613, the power spectrum of the BAT light curve shows a modest significance peak near 151 days. However, this is not consistent with the results of La Parola et al. (2014) who instead find a 118.5 ± 0.8 d period, also from BAT data. The analysis of La Parola et al. (2014) differs from ours in that they use a folding analysis, and also only selected 200 day long sections of the light curve centered on apparent outbursts in the light curve. Our analysis of the same time ranges

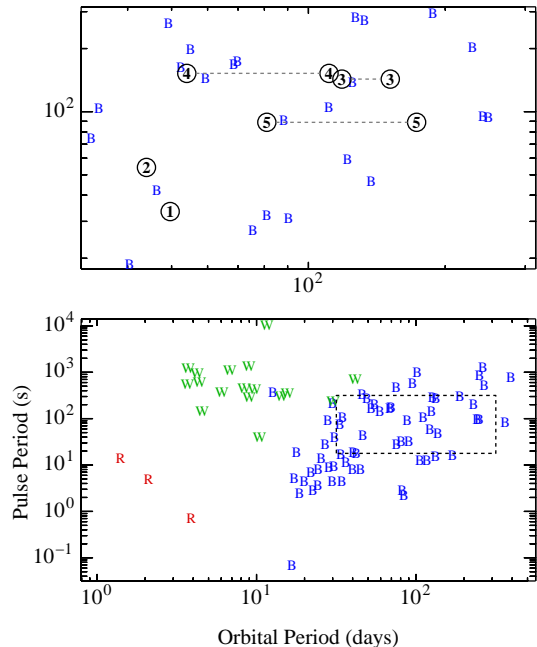


Figure 27. Bottom panel: Pulse period vs. orbital period for high-mass X-ray binaries. “B” = Be star systems, “W” = sources accreting from a stellar wind, “R” = sources thought to contain primary stars at least close to filling their Roche lobes. Top panel: Region of the pulse period vs. orbital period diagram covering the sources discussed in this paper. The plot area corresponds to the dashed box in the bottom panel. The known or possible parameters are indicated with the circled numbers: 1 - IGR J14488-5942; $P_{orb} = 49.64$ d, $P_{pulse} = 33.4$ s (this work); 2 - AX J1700.2-4220; $P_{orb} = 44.02$ d, $P_{pulse} = 54$ s (Markwardt et al. 2010); 3 - *Swift* J1816.7-1613; $P_{orb} = 118.5$ days (La Parola et al. 2014) or 151.1 days (this work), $P_{pulse} = 143$ s (Halpern & Gotthelf 2008; Krimm et al. 2013); 4 - AX J1820.5-1434; $P_{orb} = 111$ days (this work) or 54 days (Segreto et al. 2013), $P_{pulse} = 152.26$ s (Kinugasa et al. 1998); 5 - XTE J1906+09; $P_{orb} = 81$ or 173 days (this work), $P_{pulse} = 89$ s (Wilson et al. 2002).

used by La Parola et al. (2014) using a power spectrum also shows its strongest peak near 118.5 days. This indicates that the difference in our results is primarily due to the use by La Parola et al. (2014) of only restricted times while we use the full light curve. We regard the orbital period of *Swift* J1816.7-1613 as not yet clearly determined. It is possible that neither the 151 day nor the 118.5 day modulations are the actual orbital period, and both may be due to non-periodic variability.

For AX J1820.5-1434, it may be possible to interpret the 111 day period as the orbital period, and the previously proposed 54 day period (Segreto et al. 2013) as being due to the detection of the harmonic of this period. However, the overall modulation seen in the folded light curve is not smooth, which may hint at more complicated behavior and possibly that the flux modulation period is not the actual orbital period of the system. Indeed, the time-sliced folded light curves (Figure 19) are suggestive of a change in modulation period from ~ 54 days to ~ 111 days after \sim MJD 55,200. Such a change in period might be analogous to that exhibited by the peculiar HMXB 4U 2206+54, where an initial apparent period of 9.6 days was later found to transition to modulation at double this period (Corbet et al. 2007a; Wang

2009; Levine et al. 2011).

In the case of XTE J1906+090, where two peaks are seen in the power spectrum, it is unclear which, if either, is the orbital period. The apparent conflict with the pulse-timing results, if one of these peaks is the orbital period, is not necessarily a problem. As noted by Wilson et al. (2002), the apparent orbital modulation of the pulse frequency was based on a single 25 day interval which would require additional data to confirm their parameters.

For Swift J1816.7-1613, AX J1820.5-1434, and XTE J1906+090, pulse timing might have the potential to allow an unambiguous determination of these sources' orbital periods (see e.g. Townsend et al. 2011). In addition, if definite optical counterparts can be determined, then long-term optical photometry might also enable detection of their orbital periods (see e.g. Charles et al. 2012, and references therein). Further, with the determination of definite optical counterparts, long-term studies of H α could be undertaken which would be a diagnostic of the Be star's decretion disk. Changes in X-ray modulation could then be investigated for connections with decretion disk properties. For example, changes in disk size for AX J1820.5-1434 could account for the factor ~ 2 change in modulation period, if the size changes result in the neutron star impacting the decretion disk either once or twice per orbit.

5. CONCLUSION

With over 11 years of all-sky observations at X-ray energies above 15 keV, the *Swift* BAT light curves provide a sensitive way of investigating the long-term variability of HMXBs. The five sources considered here demonstrate the wide diversity of different types of long-period modulation that can be exhibited by HMXBs. In two cases (IGR J14488-5942 and AX J1700.2-4220), orbital periods can clearly be determined, which are important to understanding the properties of these systems. In the three other systems, while periodic or quasi-periodic long-term variation is seen, its interpretation is less clear. It is possible that none of these systems are exhibiting orbital modulation of their X-ray fluxes, and that more complicated variability is occurring. For these systems, the continued accumulation of long-term light curves and other types of observations, including at other wavelengths, will be important to determining the physical driving mechanism(s) behind the variability.

We thank Colleen Wilson-Hodge for useful discussions on XTE J1906+090. We thank two anonymous referees for helpful comments. This work was supported by NASA grant 14-ADAP14-0167. JBC was supported by an appointment to the NASA Postdoctoral Program at the Goddard Space Flight Center administered by Universities Space Research Association through a contract with NASA.

REFERENCES

- Anderson, G. E., Gaensler, B. M., Kaplan, D. L., et al. 2014, *ApJS*, 212, 13
- Baluev, R. V. 2008, *MNRAS*, 385, 1279
- Barthelmy, S. D., Barbier, L. M., Cummings, J. R., et al. 2005, *Space Sci. Rev.*, 120, 143
- Baumgartner, W. H., Tueller, J., Markwardt, C. B., et al. 2013, *ApJS*, 207, 19
- Bird, A. J., Barlow, E. J., Bassani, L., et al. 2004, *ApJ*, 607, L33
- Bird, A. J., Bazzano, A., Bassani, L., et al. 2010, *ApJS*, 186, 1
- Bucheri, R., Bennett, K., Bignami, G. F., et al. 1983, *A&A*, 128, 245
- Campana, S., Israel, G., & Stella, L. 1999, *A&A*, 352, L91
- Capaldi, M., Perri, M., Saija, B., Tamburelli, F., & Angelini, L. 2005, https://swift.gsfc.nasa.gov/analysis/xrt_swgguide_v1.2.pdf
- Charles, P. A., & Coe, M. J. 2006, *Compact stellar X-ray sources*, 39, 215
- Charles, P. A., Kotze, M. M., & Rajoelimanana, A. 2012, *New Horizons in Time Domain Astronomy*, 285, 23
- Chaty, S. 2010, *American Institute of Physics Conference Series*, 1314, 277
- Cheng, Z.-Q., Shao, Y., & Li, X.-D. 2014, *ApJ*, 786, 128
- Cochran, W. G. 1937, *Supplement to the Journal of the Royal Statistical Society*, 4, 102
- Cochran, W. G. 1954, *Biometrics*, 10, 101
- Coleiro, A., Chaty, S., Zurita Heras, J. A., Rahoui, F., & Tomsick, J. A. 2013, *A&A*, 560, A108
- Coley, J. B., Corbet, R. H. D., & Krimm, H. A. 2015, *ApJ*, 808, 140
- Corbet, R. H. D. 1984, *A&A*, 141, 91
- Corbet, R. H. D. 1986, *MNRAS*, 220, 1047
- Corbet, R. H. D., Markwardt, C. B., & Tueller, J. 2007, *ApJ*, 655, 458
- Corbet, R., Markwardt, C., Barbier, L., et al. 2007, *Progress of Theoretical Physics Supplement*, 169, 200
- Corbet, R. H. D., Sokolowski, J. L., Mukai, K., Markwardt, C. B., & Tueller, J. 2008, *ApJ*, 675, 1424-1435
- Corbet, R. H. D., Krimm, H. A., & Skinner, G. K. 2010a, *The Astronomer's Telegram*, 2559, 1
- Corbet, R. H. D., Barthelmy, S. D., Baumgartner, W. H., et al. 2010b, *The Astronomer's Telegram*, 2598, 1
- Corbet, R. H. D., & Krimm, H. A. 2013, *ApJ*, 778, 45
- Corbet, R. H. D., & Krimm, H. A. 2014, *The Astronomer's Telegram*, 6253, 1
- Gehrels, N., Chincarini, G., Giommi, P., et al. 2004, *ApJ*, 611, 1005
- Gögüs, E., Patel, S. K., Wilson, C. A., et al. 2005, *ApJ*, 632, 1069
- Halpern, J. P., & Gotthelf, E. V. 2008, *The Astronomer's Telegram*, 1457, 1
- Horne, J. H., & Baliunas, S. L. 1986, *ApJ*, 302, 757
- Israel, G. L., & Stella, L. 1996, *ApJ*, 468, 369
- Kaur, R., Wijnands, R., Paul, B., Patruno, A., & Degenaar, N. 2010, *MNRAS*, 402, 2388
- Kinugasa, K., Torii, K., Hashimoto, Y., et al. 1998, *ApJ*, 495, 435
- Knigge, C., Coe, M. J., & Podsiadlowski, P. 2011, *Nature*, 479, 372
- Koen, C. 1990, *ApJ*, 348, 700
- Kretschmar, P., Nespoli, E., Reig, P., & Anders, F. 2012, *Proceedings of "An INTEGRAL view of the high-energy sky (the first 10 years)" - 9th INTEGRAL Workshop and celebration of the 10th anniversary of the launch (INTEGRAL 2012). 15-19 October 2012. Bibliothèque Nationale de France, Paris, France. Published online at <http://pos.sissa.it/cgi-bin/reader/conf.cgi?confid=176>, id.16, 16*
- Krimm, H. A., Barthelmy, S. D., Baumgartner, W., et al. 2008, *The Astronomer's Telegram*, 1456, 1
- Krimm, H. A., Holland, S. T., Corbet, R. H. D., et al. 2013, *ApJS*, 209, 14
- Landi, R., Masetti, N., Capitanio, F., Fiocchi, M., & Bird, A. J. 2009, *The Astronomer's Telegram*, 2355, 1
- La Parola, V., Segreto, A., Cusumano, G., et al. 2014, *MNRAS*, 445, L119
- Levine, A. M., Bradt, H., Cui, W., et al. 1996, *ApJ*, 469, L33
- Levine, A. M., Bradt, H. V., Chakrabarty, D., Corbet, R. H. D., & Harris, R. J. 2011, *ApJS*, 196, 6
- Lutovinov, A., Walter, R., Belanger, G., et al. 2003, *The Astronomer's Telegram*, 155, 1
- Lutovinov, A., Revnivtsev, M., Gilfanov, M., et al. 2005, *A&A*, 444, 821
- Marcu-Cheatham, D. M., Pottschmidt, K., Kühnel, M., et al. 2015, *ApJ*, 815, 44
- Markwardt, C. B., Baumgartner, W. H., Skinner, G. K., & Corbet, R. H. D. 2010, *The Astronomer's Telegram*, 2564, 1
- Marsden, D., Gruber, D. E., Heindl, W. A., Pelling, M. R., & Rothschild, R. E. 1998, *ApJ*, 502, L129
- Masetti, N., Morelli, L., Palazzi, E., et al. 2006, *The Astronomer's Telegram*, 783, 1
- Matsuoka, M., Kawasaki, K., Ueno, S., et al. 2009, *PASJ*, 61, 999
- Monageng, I. M., McBride, V. A., Coe, M. J., Steele, I. A., & Reig, P. 2017, *MNRAS*, 464, 572
- Negueruela, I., & Schurch, M. P. E. 2007, *A&A*, 461, 631
- Ogilvie, G. I. 2008, *MNRAS*, 388, 1372
- Okazaki, A. T. 1991, *PASJ*, 43, 75
- Okazaki, A. T. 2016, *Bright Emissaries: Be Stars as Messengers of Star-Disk Physics*, 506, 3
- Orlandini, M., & Frontera, F. 2008, *The Astronomer's Telegram*, 1462, 1
- Porter, J. M., & Rivinius, T. 2003, *PASP*, 115, 1153
- Rajoelimanana, A. F., Charles, P. A., & Udalski, A. 2011, *MNRAS*, 413, 1600
- Reig, P., Słowikowska, A., Zezas, A., & Blay, P. 2010, *MNRAS*, 401, 55
- Reig, P. 2011, *Ap&SS*, 332, 1
- Reig, P., Nersesian, A., Zezas, A., Gkouvelis, L., & Coe, M. J. 2016, *A&A*, 590, A122
- Rivinius, T., Carciofi, A. C., & Martayan, C. 2013, *A&A Rev.*, 21, 69
- Rodriguez, J., Tomsick, J. A., & Bodaghee, A. 2010, *A&A*, 517, A14
- Scargle, J. D. 1982, *ApJ*, 263, 835
- Scargle, J. D. 1989, *ApJ*, 343, 874
- Segreto, A., La Parola, V., Cusumano, G., et al. 2013, *A&A*, 558, A99
- Sugizaki, M., Mitsuda, K., Kaneda, H., et al. 2001, *ApJS*, 134, 77
- Süveges, M. 2014, *MNRAS*, 440, 2099
- Swank, J., & Markwardt, C. 2001, *New Century of X-ray Astronomy*, 251, 94
- Townsend, L. J., Coe, M. J., Corbet, R. H. D., & Hill, A. B. 2011, *MNRAS*, 416, 1556
- Tueller, J., Baumgartner, W. H., Markwardt, C. B., et al. 2010, *ApJS*, 186, 378
- VanderPlas, J. T. 2017, [arXiv:1703.09824](https://arxiv.org/abs/1703.09824)
- Vaughan, S. 2005, *A&A*, 431, 391
- Walter, R., & Zurita Heras, J. 2007, *A&A*, 476, 335
- Walter, R., Lutovinov, A. A., Bozzo, E., & Tsygankov, S. S. 2015, *A&A Rev.*, 23, 2
- Wang, W. 2009, *MNRAS*, 398, 1428
- Wilson, C. A., Finger, M. H., Gögüs, E., Woods, P. M., & Kouveliotou, C. 2002, *ApJ*, 565, 1150
- Wilson, C. A., Finger, M. H., Coe, M. J., & Negueruela, I. 2003, *ApJ*, 584, 996
- Wilson-Hodge, C. A., Case, G. L., Cherry, M. L., et al. 2012, *ApJS*, 201, 33